Catalysis Today 166 (2011) 129–134

Contents lists available at ScienceDirect

Catalysis Today

journal homepage: www.elsevier.com/locate/cattod

Synthesis and characterization of ZnO and ZnO:Al by spray pyrolysis with high photocatalytic properties

M. Bizarro*, A. Sánchez-Arzate, I. Garduño-Wilches, J.C. Alonso, A. Ortiz

Instituto de Investigaciones en Materiales, Universidad Nacional Autónoma de México, A.P. 70-360, Coyoacán C.P. 04510 D.F., Mexico

ARTICLE INFO

Article history:
Available online 1 September 2010

Keywords:
Zinc oxide
Photocatalysis
Spray pyrolysis
Thin films

ABSTRACT

The pneumatic spray pyrolysis technique was used to deposit zinc oxide and aluminum doped zinc oxide films. X-ray diffraction (XRD), scanning electron microscopy (SEM), atomic force microscopy (AFM), and optical transmission were used to characterize the films and their photocatalytic activities were measured by the degradation of an organic dye under ultraviolet irradiation. A thickness-based rate constant was calculated for both, undoped and Al-doped thin films, obtaining values of k_t(ZnO) = 0.25 and k_t(ZnO:Al) = 0.32 h^{-1} μm^{-1}, respectively, which resulted higher than that of a TiO_2 film (k_t = 0.21 h^{-1} μm^{-1}). The stability of the films was also evaluated by the repetition of the degradation test three times. A slight decrease in the activity was observed after the third cycle particularly for the doped film. These results along with the characterization results show that the incorporation of aluminum to the zinc oxide matrix produce a slight increase in the optical band gap of ZnO:Al (3.26 eV) compared to the pure ZnO film (3.23 eV), and favors the formation of surface structures that contributed to enhance the photocatalytic activity.

1. Introduction

Zinc oxide is an important wide band gap semiconductor material, which has been used for several applications such as transparent conductors, solar cell windows, gas sensors and photovoltaic devices [1,2]. Recently, ZnO in different forms such as powders [3–7], nanoparticles [8–11], nanoplatelets [12], plates [13] and thin films [14–18] has attracted much attention as photocatalyst for photodegradation of pollutants in water. Photocatalytic materials have become a promising alternative for environmental remediation [19] because they are able to degrade several organic compounds in a more efficient way than other processes, such as biodegradation techniques [20]; thus, they constitute an alternative to eliminate pollutants in water and air [21]. Particularly, the water pollution problem needs urgent attention, because excessive waste water from industrial use contains toxic compounds which are recalcitrant and not biodegradable, like the dyes used in the textile industry [22]. The interest in ZnO is because it is a low cost alternative photocatalyst with photodegradation capacity comparable and in some cases better than that of titanium dioxide (TiO_2), which is one of the most efficient photocatalyst for degradation of organics in aqueous solutions [3–7,11–15,18].

Most of the studies concerning the photodegradation of organic compounds using ZnO have been carried out with suspensions of fine powdered ZnO in aqueous solutions [3–11]. Although the use of fine powders increases the photocatalytic efficiency due to the high effective surface area of the material, for water treatment applications the drawback is that they are hard to filter, recover and recycle, and they can even produce environmental hazards [23]. In order to avoid this problem it is convenient to use the photocatalyst immobilized as a thin film [14–18], because in this way separation of the catalyst from the clean water is avoided, reducing processing time and costs. The drawback of a supported catalyst lies in the diminution of the surface area, therefore the production of rough, porous and/or nanostructured films is quite important. A simple and low cost method to obtain ZnO films is by spray pyrolysis, which does not require vacuum conditions, and by the manipulation of the different deposition parameters, one can control the microstructure and surface features on the films [24–27]. In addition, this technique allows doping ZnO easily by adding the impurities to the precursor solution. It has been reported that controllable n-type doping is easily achieved by substituting Zn with group-III elements such as aluminum [1]. This kind of doping has been applied for the production of transparent conducting oxide films [28,29]. However, ZnO:Al has not yet been studied extensively as a photocatalyst. In the case of TiO_2, doping with elements such as N, Fe, C, among others, has been used to reduce the bandgap

* Corresponding author at: Instituto de Investigaciones en Materiales, Universidad Nacional Autónoma de México, Circuito Exterior S/N, C.P. 04510, Mexico City, Mexico. Tel.: +52 55 56224770x45671; fax: +52 55 56161251.
E-mail address: monserrat@iim.unam.mx (M. Bizarro).

0920-5861/$ – see front matter © 2010 Elsevier B.V. All rights reserved.
doi:10.1016/j.cattod.2010.08.005

of the semiconductor and make possible the absorption of visible light.

In the present work, ZnO and ZnO:Al films with high photocatalytic activity have been produced by spray pyrolysis to degrade a typical organic dye; their photocatalytic efficiencies were compared to that obtained for a TiO_2 film.

2. Experimental details

Zinc oxide films were obtained by the spray pyrolysis technique employing a home-made pneumatic spray system (shown in Fig. 1) which uses an air atomizing 1/4 JAU-SS nozzle, from Spraying Systems Co. A 0.2 M solution of zinc acetate ($Zn(CH_3COO)_2{\cdot}2H_2O$, 98% purity from Sigma–Aldrich) was dissolved in deionized water ($\rho \geq 15\,M\Omega\,cm$). Aluminum doping was achieved by adding 5 at% of aluminum chloride ($AlCl_3{\cdot}6H_2O$, 99% purity from Aldrich) to the previous solution. The films were formed at a substrate temperature of 550 °C with a gas flow rate of 9 L/min and a solution flow rate of 18.2 mL/min. The deposition time was of 10 min in each case. The nozzle was kept at a constant distance from the substrate (32 cm) for all the samples. The substrates used to deposit the films were pyrex glass slides of 2.5 cm × 1.25 cm × 0.01 cm, that were cleaned consecutively with trichloroethylene, acetone, and methanol for 5 min in an ultrasonic bath.

To compare the photocatalytic efficiency of pure and Al-doped ZnO films, TiO_2 films were prepared by ultrasonic spray pyrolysis [30], using titanium(IV) oxide acetylacetonate ($TiO(CH_3COH{=}C(O-)CH_3)_2$, 99% purity from Aldrich) with a concentration of 0.075 M dissolved in methanol. The deposition temperature was 550 °C and the director gas and carrier gas flow rates were 8 L/min and 11 mL/min, respectively.

The films were analyzed by X-ray diffraction (D8 Advance Bruker) using the Cu $K\alpha_1$ wavelength (1.54056 Å). The morphology of the films was studied by Scanning Electron Microscopy (SEM) (Leyca Cambridge 400) and by atomic force microscopy (Jeol, JSPM-4210). To observe the samples with SEM, a gold layer of 5 nm was sputtered (Cressington Sputter Coater 108 auto). The thickness and roughness of the films were measured with a profilometer (Sloan DekTac IIA). The optical transmission of the films was measured with a double beam UV-vis spectrophotometer (Perkin Elmer Lambda 35), using air in the reference beam.

The photocatalytic activity of the films was studied by the degradation of an aqueous solution 10^{-5} M of methyl orange dye ($C_{14}H_{14}N_3SO_3Na$, 85% from Sigma–Aldrich) with a pH of 6.8, measured with a Horiba B-213 Twin pH-meter. The pH of the solutions remained constant after de degradation. The methyl orange dye (MO) was chosen as a test compound because is a typical pollutant in waste water from textile industry [22]; besides, the degradation of this kind of dyes is easily followed by absorption spectroscopy. Two identical samples were placed back to back in order to have the catalyst film in both sides when immersed in 10 mL of the dye solution contained in a glass vial. The solution covered the films completely and the vials were placed at a distance of 2 cm from the UV lamp. The emission of the UV lamp is centered at 380 nm and has a power of 7 W. A schematic representation of the reactor is shown in Fig. 2. The absorption spectra of the solutions were recorded as a function of the irradiation time with a UV-vis spectrophotometer (Perkin Elmer Lambda 35) from 190 nm to 800 nm.

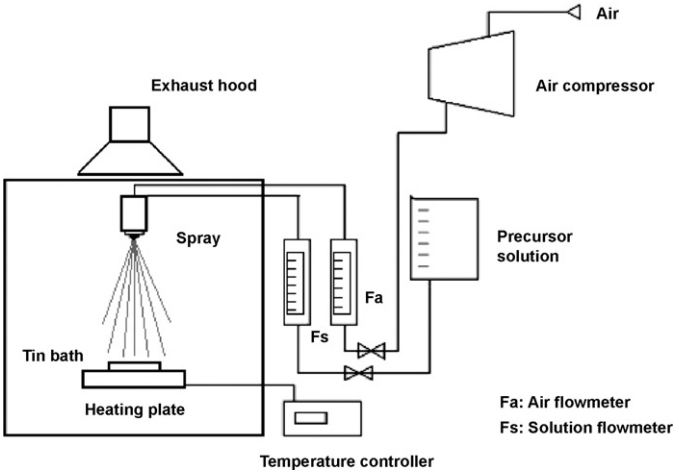

Fig. 1. Diagram of the pneumatic spray pyrolysis deposition system.

3. Results

3.1. Microstructure

Although the deposition conditions for pure and aluminum doped ZnO films were similar, the film growth resulted different starting from their color and texture. ZnO films were more white and smooth than the ZnO:Al. For the same deposition times their average thicknesses were 1.95 μm and 2.24 μm, respectively. The roughness was also measured giving values of 0.1 μm for ZnO and 0.7 μm for ZnO:Al, as expected just by their physical aspect at a glance.

The crystalline structure of the films analyzed by X-ray diffraction showed that pure and doped ZnO present the wurtzite hexagonal structure, indicated by the ICDD data base PDF 01-089-1397 and is presented in Fig. 3. The aluminum doped film did not show any lattice distortion, which is an indicative that either the aluminum is in a very small proportion (under the limit of detection of the apparatus) or part of it is incorporating in an amorphous phase. The grain size was estimated using Scherrer's formula applied to the (1 0 0) peak, giving values of ~50 nm and ~80 nm for ZnO and ZnO:Al, respectively. So the aluminum favored the crystal growth. In addition, the SEM images shown in Fig. 4, indicate a drastic change in the surface morphology that goes from small tri-

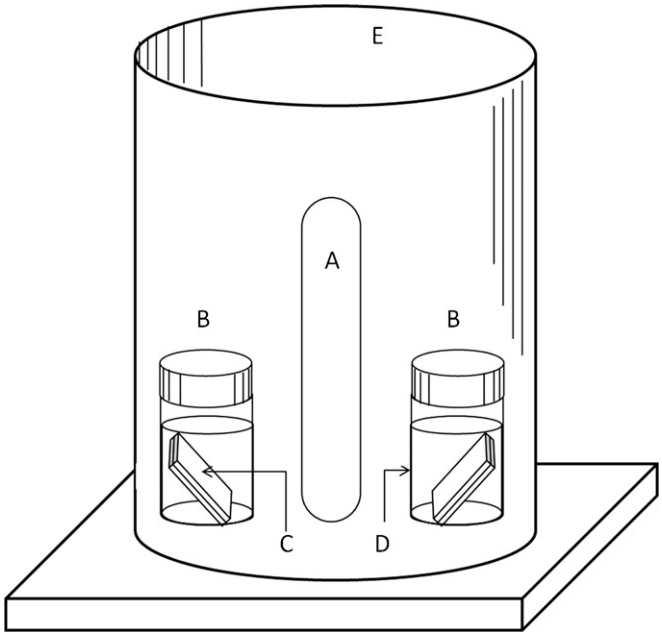

Fig. 2. Schematic representation of the photocatalytic reactor, where (A) is the UV lamp, (B) are the glass containers, (C) are the catalyst films, (D) is the test solution (methyl orange in this case) and (E) is the casing.

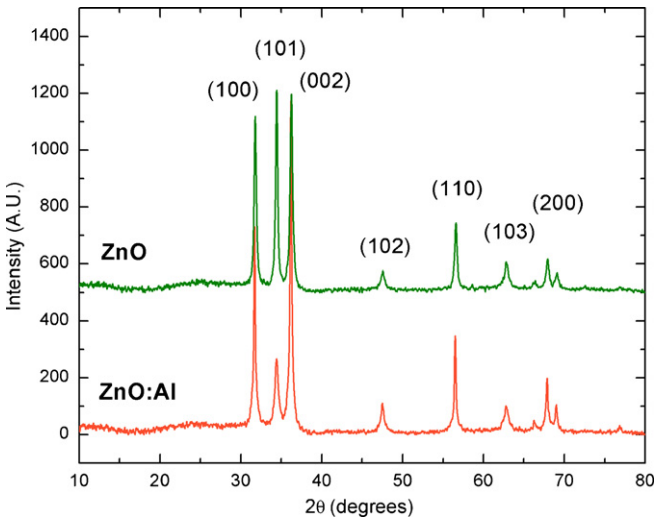

Fig. 3. XRD spectra of ZnO and ZnO:Al films showing the wurtzite phase. Any other phase due to the aluminum incorporation is present.

angular plates in ZnO films (Fig. 4a) to big rounded shapes in ZnO:Al films (Fig. 4b). These rounded features appeared on the surface and are around 50 μm in diameter, contributing in a great manner with the roughness of the film. Besides, they seem to be very porous, a characteristic that plays an important role in photocatalysis [31].

Fig. 5 shows AFM images with scanning areas of 5 μm × 5 μm of the undoped (Fig. 4a) and doped (Fig. 4b) films. Both samples exhibit different surface morphologies and the change in their roughness is also appreciated. It is worth mentioning that the scan of the doped film was performed on the flattest area, discarding the big rounded features on the surface that the AFM tip was not able to measure. In addition, the surface of the TiO_2 film is also presented (Fig. 4c), where it is appreciated a smaller particle size. A change in ZnO surface morphology with Al doping was also reported by Ding et al. who also found a roughness increase with increasing Al content [32].

3.2. Optical properties

The optical transmittance of the pure and doped ZnO films was also measured and analyzed in order to obtain their optical band gaps. The absorption coefficient (α) was obtained using the Lambert–Beer equation:

$$I = I_0\, e^{-\alpha d}$$

where I_0 and I are the intensities of the incident and the transmitted light beam, respectively and d the film thickness. Considering that ZnO has a direct band gap, a plot of $(\alpha h\nu)^2$ versus the photon energy was used to obtain, by a linear fit, the optical band gap of each material. As it can be seen in Fig. 6, the optical band gap of the Al-doped sample is slightly larger than that of the pure ZnO film. This result is in agreement with those obtained by other authors

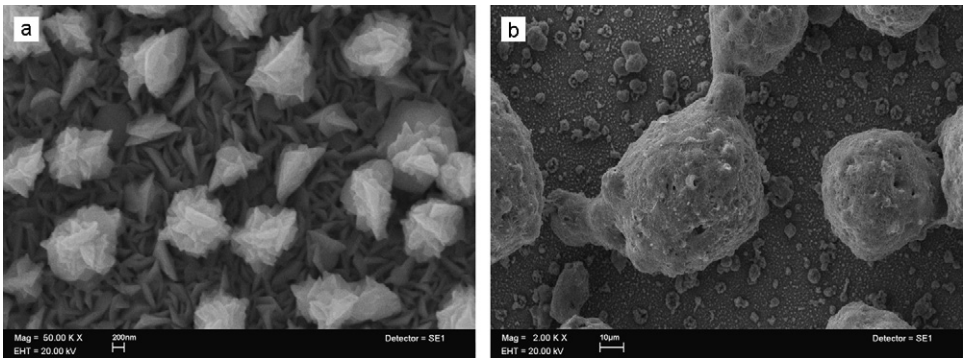

Fig. 4. SEM images of the surface morphology of ZnO (a) and ZnO:Al (b) films.

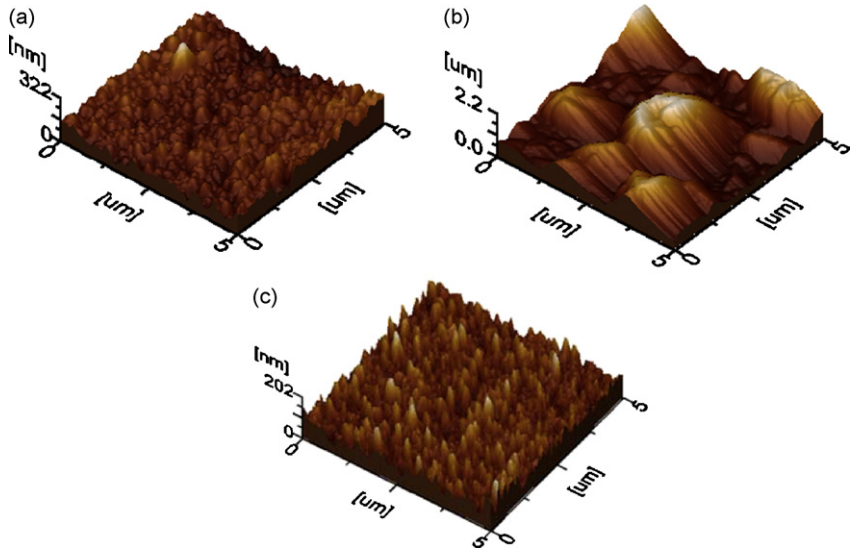

Fig. 5. AFM images of ZnO (a) and Al-doped ZnO (b) films show different surface texture. TiO_2 suface shows a smaller particle size (c).

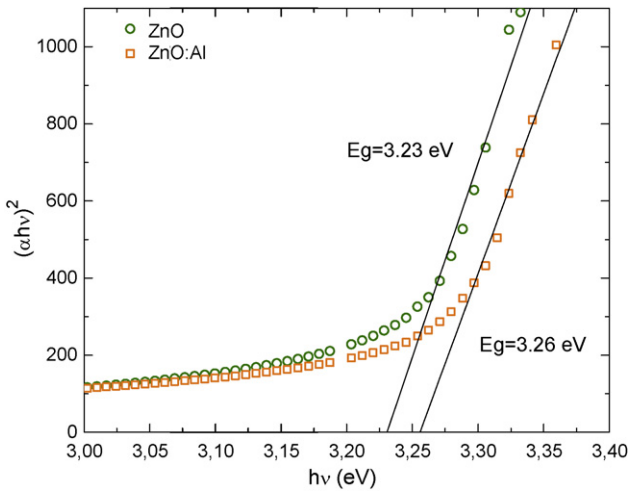

Fig. 6. Optical band gap of ZnO and ZnO:Al films obtained by optical transmission measurements. An increase in the gap is show for the film with Al.

[28,32,33], and can be explained by the Moss–Burstein effect, that states that the blue-shift of the optical band gap of semiconductors is due to the introduction of impurities that fill states at the bottom of the conduction band. As the Pauli's exclusion principle forbids a double occupied state and the optical transitions are vertical, the electrons in the valence band require higher energy to be excited to states in the conduction band (Fig. 7) [34]. This implies that an improvement of the photocatalytic reactions by the addition of aluminum cannot be explained by a reduction of the gap, as it has been suggested by Shahjahan et al. [17]. Rather, it could be attributed to the extra charge provided by the aluminum impurities.

3.3. Photocatalysis

The degradation of the methyl orange dye was measured by following the evolution of the intensity of the absorption band centered at 464 nm, as a function of the illumination time, as it is shown in Fig. 8. The concentrations ratio (C/C_0) was calculated to evaluate the degradation of the dye. As it is appreciated in Fig. 9, the aluminum doped ZnO film degraded almost all the dye (about a 90%) in only 3 h, while the undoped ZnO film reached the same value after almost 5 h of illumination. It is clearly seen that the presence of 5% of aluminum in the ZnO matrix accelerates the photocatalytic process. For comparative purposes Fig. 9 also presents the degradation of methyl orange by the TiO_2 film with anatase crystal structure. This TiO_2 film reached a 90% of the dye removal in 7.5 h.

The kinetics of the reaction was obtained by plotting the natural logarithm of the concentration ratios versus the irradiation time. Straight lines were obtained, indicating that the reactions are of first order. As it is shown in Fig. 10, the sample with the highest rate of reaction is the one that contains aluminum, giving a $k = 0.73\ h^{-1}$, while ZnO gave a $k = 0.49\ h^{-1}$; this means that the incorporation of aluminum in the film, increases the photocatalytic efficiency. To provide a better comparison between each film, a thickness-based rate constant (k_t) was obtained to eliminate the effect of the difference in thickness of the different samples. These values are presented in Table 1, where it is clear that the ZnO:Al film has the highest photocatalytic efficiency. In spite the k_t gives an idea of the films performance, it is not completely rigorous; a more detailed study of the morphologies and structures of the films is necessary to understand their contributions to the photocatalysis, as it has been observed by Ali et al. [18].

To study the stability of the pure and doped ZnO films, the photocatalysis experiments were repeated three times, using in each cycle new dye solution with the same initial concentration. Fig. 11 shows the rate of reaction achieved in the different cycles. It can be observed a small diminution of the rate constant in the second cycle for both samples; but in the third repetition the decrease in the photocatalytic activity is more notable for the Al-doped ZnO film. More work needs to be done in order to improve the stability of ZnO:Al films.

4. Discussion

All the previous results indicate a change in the physical and chemical properties of ZnO when it is doped with aluminum. Despite that the X-ray analysis does not show any lattice distor-

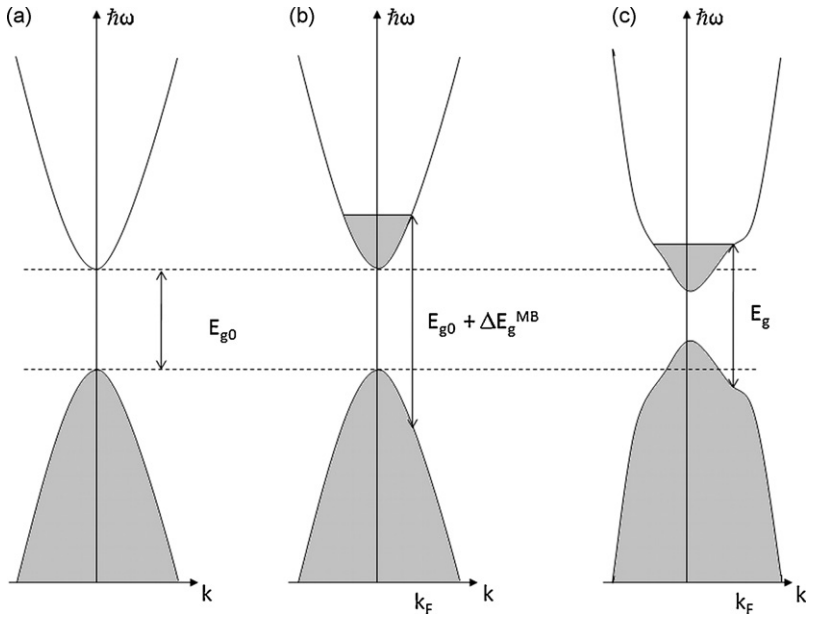

Fig. 7. Schematic band structure of ZnO. (a) In the pure ZnO, the optical bandgap is the energy separation E_{g0} between the band edges; (b) in the doped semiconductor, the lowest states in the conduction band are blocked so that the optical gap is widened by the Moss–Burstein effect ΔE_g^{MB}; (c) the bandgap widening is counteracted by a narrowing caused by the correlated motion of the charge carriers and by their scattering against ionized impurities [33].

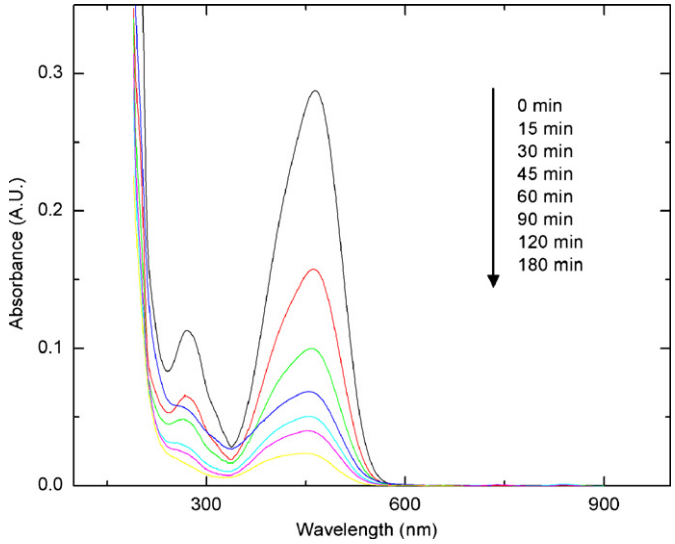

Fig. 8. Evolution of the absorption spectra of MO dye in the presence of the photocatalyst and UV light.

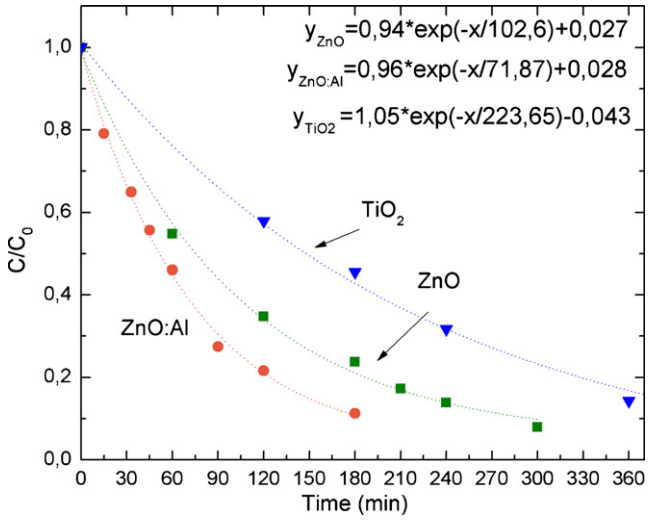

Fig. 9. Degradation of the MO dye by ZnO and ZnO:Al films and its comparison between a TiO_2 films.

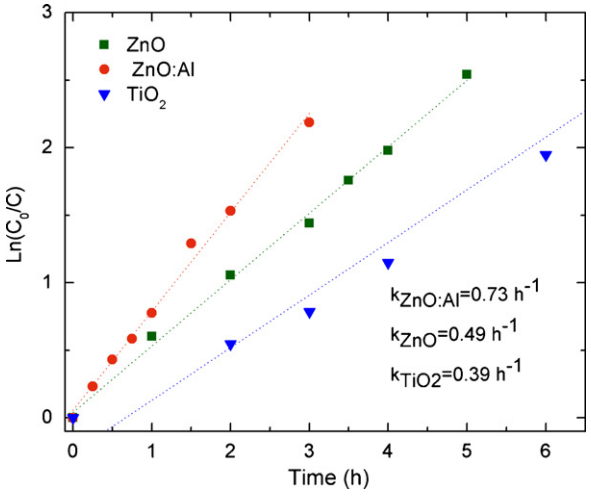

Fig. 10. Comparison of the rates of reaction of ZnO, ZnO:Al and TiO_2 films, showing the highest activity of the Al-doped ZnO film.

Table 1
Rate of reaction and thickness-based rate of reaction of the different films.

Sample	k (h^{-1})	k_t (h^{-1} μm^{-1})	Time to degrade 90% of the dye (h)
TiO_2	0.39	0.21	7.5
ZnO	0.49	0.25	4.75
ZnO:Al	0.73	0.32	3

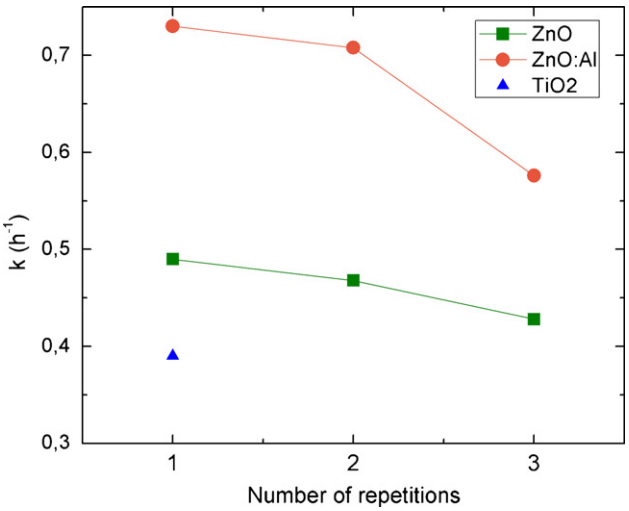

Fig. 11. Stability of the films after three cycles of dye degradation.

tion in the spectrum of the doped films, the surface morphology was modified in a great manner by the introduction of aluminum. This change in morphology plays an important role in the photocatalytic activity of the film, that increases the rate of reaction almost a 50% of the obtained for the pure ZnO. The larger roughness, as well as the big porous features on the surface, contributes to this improvement.

Doping of TiO_2 with elements such as N, Fe and C has been used to decrease the bandgap and use visible light for the photocatalytic process. However, in this case, the incorporation of aluminum in the ZnO matrix gives the opposite effect, a slight widening of the bandgap. It is well established that the substitution of group III elements (like aluminum) on the Zn sites, produce n-type ZnO. Generally speaking, Al on Zn sites can form shallow donors in ZnO. In fact, ZnO with a wurtzite structure is naturally an n-type semiconductor because of deviation from stoichiometry due to the presence of intrinsic defects such as O vacancies (V_O) and Zn interstitials (Zn_i) [2]. So the substitutional aluminum impurities provide extra charge that is available for the photochemical reactions. In this case, the photocatalytic films were immersed in an aqueous solution containing the dye molecule. When this system (semiconductor + water + dye) is illuminated with UV light, the generation of electron–hole pairs begins. The produced holes (h^+) react with H_2O molecules forming $OH^\bullet$ radicals and H^+. The generated electrons (e^-) react with O_2 molecules to form $O_2^{\bullet -}$ radicals. These products will form H_2O_2 molecules that, joint with $OH^\bullet$ radicals, will lead to the dye mineralization [35]. The formation of H_2O_2 occurs in a more efficient way in ZnO:Al than in ZnO films, giving as a result a faster discoloration of the dye. This mechanism is even more efficient in ZnO than in TiO_2.

5. Conclusions

Pure and aluminum doped ZnO films were deposited by the spray pyrolysis technique. The addition of 5 at% of aluminum to the start solution modified the morphology of the films and improved

the photocatalytic activity of ZnO, reducing the discoloration time of the methyl orange dye from 5 h to 3 h under UV illumination. The photocatalytic efficiency of these films was greater than the activity achieved by a TiO_2 film grown under similar conditions, giving a thickness-based rate constant of 0.21 (TiO_2) < 0.25 (ZnO) < 0.32 (ZnO:Al) h^{-1} μm^{-1}. ZnO and ZnO:Al films were reproducible and stable, although a small decrease in the photocatalytic activity was observed after the third cycle of dye degradation. The optical bandgap resulted slightly greater for the Al-doped film, as explained by the Moss–Burstein effect, so the photocatalytic activity cannot be attributed to a gap diminution, rather it could be attributed to the extra charge provided by the aluminum impurities.

Acknowledgements

The authors wish to thank Omar Novelo, Adriana Tejeda, Carlos Flores and Oralia Jiménez for technical support and Dr. Francisco Sánchez and Dr. Estrella Ramos for the revision and improvement of the manuscript. This work was supported by DGAPA under project IN-116109.

References

[1] S.J. Pearton, D.P. Norton, K. Ip, Y.W. Heo, T. Steiner, Prog. Mater. Sci. 50 (2005) 293–340.
[2] H. Markoç, Û. Özgûr, Zinc Oxide, Fundamentals, Materials and Device Technology, Wiley-VCH Verlag, Weinheim, 2009.
[3] B. Dindar, S. Içli., J. Photochem. Photobiol. A 140 (2001) 263–268.
[4] D. Li, H. Haneda, Chemosphere 51 (2003) 129–137.
[5] N. Daneshvarm, D. Salari, A.R. Khataee, J. Photochem. Photobiol. A 162 (2004) 317–322.
[6] S.K. Kansal, M. Singh, D. Sud, J. Hazard. Mater. 141 (2007) 581–590.
[7] H. Fu, T. Xu, S. Zhu, Y. Zhu, Environ. Sci. Technol. 42 (2008) 8064–8069.
[8] H.-F. Lin, S.-C. Liao, S.-W. Hung, J. Photochem. Photobiol. A 174 (2005) 82–87.
[9] C. Hariharan, Appl. Catal. A 304 (2006) 55–61.
[10] K.G. Kanade, B.B. Kale, J.-O. Baeg, S.M. Lee, C.W. Lee, S.-J. Moon, H. Chang, Mater. Chem. Phys. 102 (2007) 98–104.
[11] R. Ullah, J. Dutta, J. Hazard. Mater. 156 (2008) 194–200.
[12] C. Ye, Y. Bando, G. Shen, D. Golberg, J. Phys. Chem. B 110 (2006) 15146–15151.
[13] E. Yassitepe, H.C. Yatmaz, C. Öztürk, K. Öztürk, C. Duran, J. Photochem. Photobiol. A 198 (2008) 1–6.
[14] A.A. Aal, S.A. Mahmoud, A.K. Aboul-Gheit, Mater. Sci. Eng. C 29 (2000) 831–835.
[15] B. Pal, M. Sharon, Mater. Chem. Phys. 76 (2002) 82–87.
[16] J.L. Yang, S.J. An, W.I. Park, G.C. Yi, W. Choi, Adv. Mater. 16 (2004) 1661–1664.
[17] M. Shahjahan, M.K.R. Khan, M.F. Hossain, S. Biswas, T. Takahashi, J. Vac. Sci. Technol. A27 (4) (2009) 885–888.
[18] A.M. Ali, E.A.C. Emanuelsson, D.A. Patterson, Appl. Catal. 97 (2010) 168–181.
[19] M.R. Hoffmann, S.T. Martin, W. Choi, D.W. Bahnemann, Chem. Rev. 95 (1995) 69–96.
[20] P. R- Gogate, A.B. Pandit, Adv. Environ. Res. 8 (2004) 501–551.
[21] C. Comninellis, A. Kapalka, S. Malato, S.A. Parsons, I. Poulios, D. Mantzavinos, J. Chem. Technol. Biotechnol. 83 (2008) 769–776.
[22] T. Robinson, G. McMullan, R. Marchant, P. Nigam, Bioresour. Technol. 77 (2001) 547–555.
[23] K. Kabra, R. Chaudhary, R.L. Sawhney, Ind. Eng. Chem. Res. 43 (2004) 7683–7696.
[24] P.S. Patil, Mater. Chem. Phys. 59 (1999) 185–198.
[25] D. Perednis, L.J. Gaukler, J. Electroceram. 14 (2005) 103–111.
[26] M.T. Htay, Y. Hashimoto, K. Ito, Jpn. J. Appl. Phys. 46 (2007) 440–448.
[27] D. Li, H. Haneda, J. Photochem. Photobiol. A 155 (2003) 171–178.
[28] S.M. Rozati, S. Akesteh, Mater. Charact. 58 (2007) 319–322.
[29] T. Schuler, M.A. Aegerter, Thin Solid Films 351 (1999) 125–131.
[30] L. Castañeda, J.C. Alonso, A. Ortiz, E. Andrade, J.M. Saniger, J.G. Bañuelos, Mater. Chem. Phys. 77 (2002) 938–944.
[31] X. Fan, X. Chen, S. Zhu, Z. Li, T. Yu, J. Ye, Z. Zou, J. Mol. Catal. A 284 (2008) 155–160.
[32] J.J. Ding, S.Y. Ma, H.X. Chen, X.F. Shi, T.T. Zhou, L.M. Mao, Physica B 404 (2009) 2439–2443.
[33] F.K. Shan, L.M. Yu, J. Eur. Ceram. Soc. 24 (2004) 1869–1872.
[34] B.E. Sernelius, K.-F. Berggren, Z.-C. Jin, I. Hamberg, C.G. Granqvist, Phys. Rev. B 37 (1988) 244–248.
[35] C.A.K. Gouvea, F. Wypych, S.G. Moraes, N. Durán, N. Nagata, P. Peralta-Zamora, Chemosphere 40 (2000) 433–440.